

Shape Memory Alloy Actuated Ankle Foot Orthosis for Reduction of Locomotion Force

Ahmad Alminnawi
Graduate School of
Engineering Science,
Osaka University
Osaka, Japan
ahmad.alminnawi@gmail.com

Yo Kobayashi
Graduate School of
Engineering Science,
Osaka University
Osaka, Japan
yo.kobayashi@me.es.osaka-u.ac.jp

Tomohiro Otani
Graduate School of
Engineering Science,
Osaka University
Osaka, Japan
otani@me.es.osaka-u.ac.jp

Masao Tanaka
Graduate School of
Engineering Science,
Osaka University
Osaka, Japan
tanaka@me.es.osaka-u.ac.jp

Abstract—Humans can be considered inefficient at walking because they are unable to achieve the theoretically ideal “zero energy cost” of steady-state locomotion that is possible for bipeds who have elastic tissues. This inefficiency is mainly due to part of the energy that is generated by the body to complete a single step being dissipated instead of being stored for use in the proceeding step. This suggests that we can improve locomotion efficiency and reduce the metabolic energy cost of walking by manipulating the elasticity of the lower limbs using exoskeletal devices [1]. However, most traditional designs use springs made from regular material that have a constant stiffness. These devices exert a linear force pattern that is not biocompatible because they do not mimic the forces of the muscles or the tendons of the human body. This paper presents an interdisciplinary study of the design of a passive–dynamic ankle foot orthosis mechanism that reduces the biological muscle force requirements during locomotion, thus reducing the metabolic energy cost of walking while maintaining biocompatibility. Shape memory alloy is used as a smart material for an actuator owing to its super-elasticity. This super-elasticity provides a nonlinear stiffness pattern that generates forces comparable to those of healthy muscles.

Keywords—ankle foot orthosis, biocompatibility, gait, locomotion, shape memory alloy

I. INTRODUCTION

A. Background

Humans spend more energy in walking than in any other daily activity [2]. It is evident that energy is wasted in walking because the muscles require chemical energy to perform both flexion and extension of the limbs [3]. Humans are considered one of the most energy-efficient animals when it comes to walking, but they do not achieve the theoretically ideal energy efficiency in steady-state walking on a level surface that is possible for bipeds who have elastic tissues [2][4].

B. Motivation

Reducing the metabolic energy used by humans in walking can lead to improved mobility and a longer duration of activity prior to fatigue. Several aspects govern the metabolic energy cost but muscles are considered the central locality for energy disbursement during active motion [5]. Reducing muscle forces would greatly reduce the amount of energy spent by the body in performing locomotion.

This work was supported by the Japan Society for the Promotion of Science under a Grant-in-Aid for Scientific Research (B) (No. 19H02112) and a Grant-in-Aid for Challenging Exploratory Research (No. 19K22878).

C. Related Studies

Prosthetics and orthoses, especially those that aid locomotion, have been around for centuries. They have been used to replace missing leg parts and to correct abnormality in the gait pattern, respectively [6]. However, passive articulated devices for the ankle joint, which provide dynamic support according to the gait phase while not requiring external energy sources to aid locomotion, are relatively new. To implement an energy storing and releasing mechanism for the ankle, the device should store energy in the stance phase and release the energy when it is most needed: the push-off phase. One important example of such orthoses is a device created by Collin et al. [2]. This device uses a spring to reduce the metabolic energy cost of the locomotion by 4.6%–9.8% for healthy individuals, and the device thus competes with active orthoses. They showed that the effectiveness of the device varies with respect to the stiffness of the used spring and concluded that there is an inverted bell curve relationship between the net metabolic energy rate and the exoskeleton spring stiffness. This gives a specific optimal range of 150 and 250 Nm/rad in which the stiffness of the spring aids the ankle in walking without affecting other aspects of the gait. However, we cannot consider the stiffness range as a goal because the stiffness of a device should be adjusted according to the user’s preferences and each person tolerates a different stiffness level, meaning that a universal optimal stiffness should not dictate the design [7][8].

The studies [4], [9] and [10] suggested that the majority of mechanical work is performed by the ankle joint whereas the knee and hip make limited contributions in thrusting the body forward and commencing the gait, which is the reason for focusing on the ankle joint for devices. One study [11] suggested that the amount of required energy is highest in the toe-off phase when the foot leaves the ground while the amount of dissipated energy is highest in the heel-strike phase when the foot comes into contact with the ground.

D. Problems

Traditionally, orthoses have elastic components of constant stiffnesses and thus provide a linear force pattern that varies directly with respect to the foot angle. In some cases, this leads to a gait that feels unnatural to the user. While walking, humans exert forces that depend on the angle of the joint but are not multiplicatively connected to a constant, meaning that the ratio of the force to the angle is usually a variable. The tendons store and release energy to protect the muscle by lengthening the muscle’s rate of activity, giving the muscle more time to dissipate energy

[12]. This means that the biological stiffness varies and, to maintain biocompatibility, the stiffnesses of the orthosis should vary accordingly.

One way of achieving the desired variable stiffness is to use active devices that control the stiffness of the exoskeleton to provide a more natural gait. However, such devices fall short in terms of their weight and size and are uncomfortable after a few hours of use. Therefore, the focus of recent studies has shifted to passively controlling the stiffness of ankle foot orthoses (AFOs).

E. Objective

The super-elasticity of shape memory alloys (SMAs) presents a mechanical stiffness variation that is comparable to the stiffness variation of healthy muscle [13] and provides a compatible force pattern. This suggests that the use of SMA will make the gait feel more natural and will allow for higher biocompatibility. Furthermore, these alloys are known to have higher energy densities than other materials, meaning that they are smaller, lighter, and more compact alternatives for conventional actuators.

The present paper thus proposes a design for a passive dynamic AFO, which is shown in Fig. 1, that utilizes the super-elastic property of SMA springs to store and release energy with respect to the foot angle and thus provide a nonlinear force pattern similar to that of healthy muscles. It is thus possible to maintain biocompatibility and a healthy gait. This AFO has the potential to reduce the locomotion force requirements by complementing the Achilles tendon in performing plantarflexion in the push-off phase. The objective of this study was to create a step-by-step procedure for the design of an AFO that maintains biocompatibility while reducing the forces required by the biological muscles during locomotion and to present an example of a study participant using the AFO. This study had two parts. First, the biomechanics of the human ankle were studied to calculate the ankle torque that should be presented to walk with a natural and healthy gait. Second, spring properties and dimensions that enable the orthosis to mimic the aforementioned gait were selected.

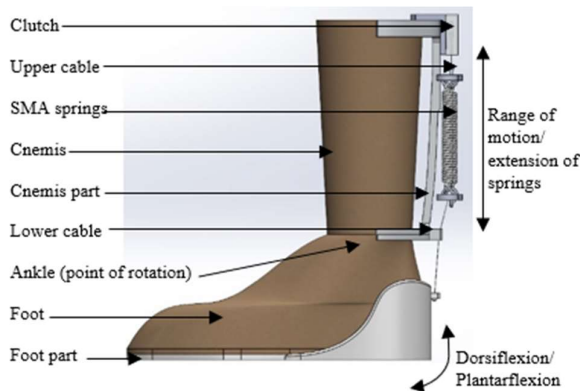


Fig. 1. Concept of the SMA AFO

II. BIOMECHANICS OF THE HUMAN GAIT

A. Objective

Before designing an AFO, the forces that are exerted by the user's muscles should be determined. These forces dictate the efficacy of the AFO and the material that should be used for each part of the device. Therefore, the objective of this section was to calculate the forces of the calf muscles during habitual walking that will be the target forces required of the AFO. These forces were determined from the torque that acts at the ankle joint of the participant, which is in turn determined from graphs of the motion (of the position, speed, and acceleration) of the lower limb segments.

B. Methodology

The device is designed to be used for community ambulation mostly on a flat and level surface. The calculations in this study thus focus on the sagittal plane. In this two-dimensional study, the forward-backward motion was set along the x-axis whereas the upward-downward motion was set along the y-axis and, by convention, the z-axes were set normal to the x-y plane.

The accelerations in the x and y directions in addition to the angular velocities about the z-axes were measured for the trunk, thigh, shank, and foot using inertial measurement units (IMUs). The IMUs were placed in accordance with the IMU-to-body alignment method presented by Vargas-Valencia [14]. The angular accelerations and angular positions were respectively differentiated and integrated with respect to time from the angular velocity. For the trunk, the IMU sensor was placed on the sacrum (S2 spinous) just below the belt of the participant. The thigh IMU was placed on the iliotibial tract 5 cm from the patella. The shank IMU was located 5 cm from the

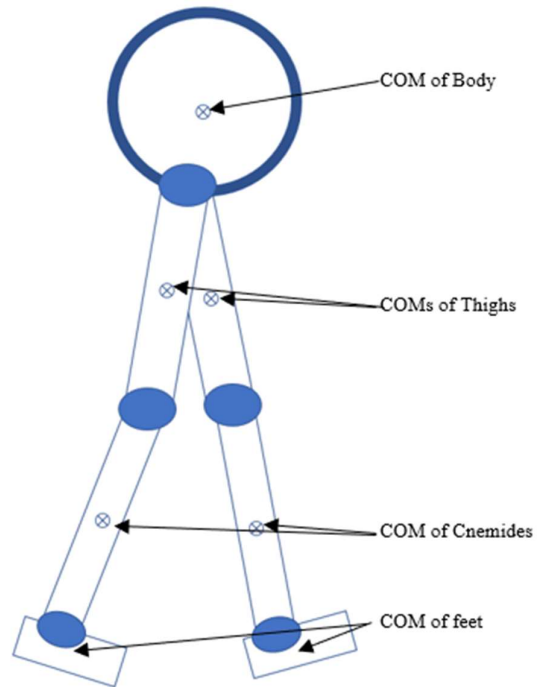


Fig. 2. Bipedal model

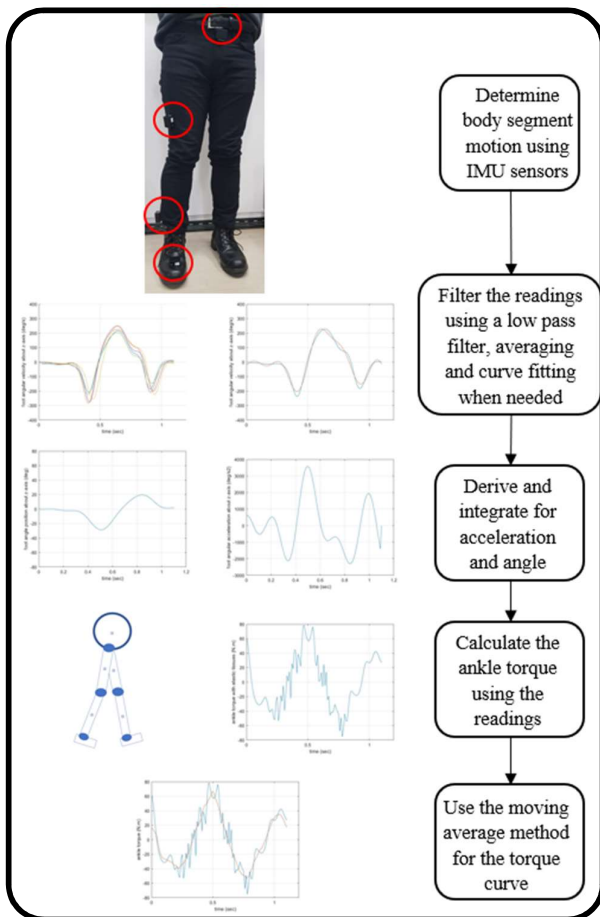


Fig. 3. Process of the biomechanical study

lateral malleolus of the fibula. Finally, the foot IMU was placed above the third and fourth metatarsal bones. It is noted that calibration using the quaternions of the IMU sensors was not conducted because the body segments did not move in three dimensions.

The experiment was performed for a male participant weighing 60 kg and standing at a height of 1.63 m twice on different days. Each experiment was preceded by two trials to verify the precision of the sensors. The participant was asked to stand still for 5 seconds, then walk 12 steps at a comfortable self-selected speed on a flat level surface, and then stand still for another 5 seconds.

The signals were refined using a series of methods. First, the signals were filtered using a low-pass 5-Hz filter to remove high-frequency noise. Second, the walking process was divided into strides starting and ending at the mid-stance phase of the right leg, and the data were averaged to produce one full gait cycle with higher accuracy that best represents the motion of body segments during walking. Third, the signals of the preceding segments were subtracted to acquire the accelerations and velocities that each joint is responsible for, which is the acceleration and velocity of each segment relative to that of its precursor. The angular velocity signals were plotted and curve-fitted before being derived to determine the angular acceleration for the removal of small disturbances.

After obtaining the instantaneous values of the accelerations and angular positions of the body segments, a

numerical simulation of human locomotion was conducted to calculate the torque at the ankle, which was smoothed using the moving average. This simulation used a bipedal model, which is shown in Fig. 2, having a point mass that represents the entire upper body (head, trunk, and upper limbs) located at the center of the chest (30 cm above the hips). The thigh and shank were modeled as cylinders while the foot was modeled as a rectangle. The ankle torque determines the amount of energy that should be stored and released by the device for the participant to move at his self-selected speed. Assumptions had to be made in calculating this torque. The mass and length of each body segment in addition to the radii of the thigh and shank were taken from literature reviews [15][16][17][18]. Figure 3 summarizes the overall process of the biomechanical study.

C. Results

The participant had an average step length of 0.65 m and walked at an average speed of 1 m/s.

Figure 4 shows the experimental results of the angular position of the foot while walking. The foot accelerations varied continuously for the participant with respect to the three axes. The angular position decreased from 0° at the beginning of the gait (in the stance phase) to -30° at plantarflexion of the toe-off phase and then increased to 20° at dorsiflexion of the heel-strike phase before returning to 0° to restart the cycle as shown in Fig. 4. The range of motion of the foot was thus 50° . These data were input into the previously mentioned bipedal model to calculate the

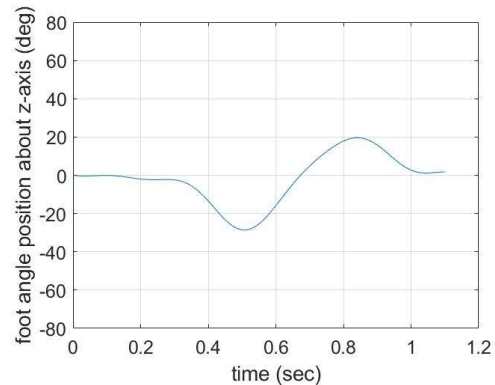


Fig. 4. Angular range of the motion of the foot

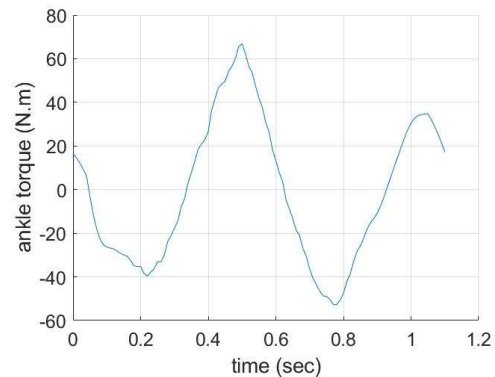


Fig. 5. Ankle torque of the gait

required torques that should be presented at the ankle joint. This torque was then adjusted according to the effect of the elastic tissues.

Figure 5 shows the experimental results of the ankle torque for walking. The maximum ankle torque was calculated to be 67 Nm, which is 112% of the mass of the participant and comparable to other findings that the maximum ankle torque of an individual (in Nm) ranges between 100% and 150% of the mass of the individual (in kg) depending on the speed of walking [19].

The AFO is intended to be compact and should aid the ankle by pulling the heel up toward the calf at push-off. The line of action of the device was thus set directly behind the heel at a distance 5.5 cm from the ankle. Therefore, the maximum force that should be supplied by the device to contribute for 100% of ankle torque is 1200 N.

III. SPRING PROPERTIES AND DIMENSIONS

SMA is a relatively new discovery first reported in the 1930s. There are two types of SMAs, namely one-way and two-way SMAs, and each type has two phases, namely the austenite (parent) and martensite (child) phases. In a one-way SMA, the austenite phase is strong, stable, and unique whereas the martensite phase is less stable and usually considered the “deformed phase” and thus can attain different shapes. In the two-way SMA, the martensite phase also has a unique shape [20]. Each phase has its own lattice structure at the atomic level, usually a face-centered cubic crystal structure for the austenite phase and a body-centered tetragonal crystal structure for the martensite phase, and the alloy can alternate between these phases when stimulated. The ability to transform between two phases gives the SMA two distinct properties, namely a shape memory effect, which is controlled by heat, and a super-elasticity (also called pseudo-elasticity), which is controlled by stress. SMAs have five distinct temperatures that are, in ascending order, $M_f < A_s < M_s < A_f < M_d$. Here, M_s and M_f denote the temperatures of the start (0%) and finish (100%) of the martensite phase upon being cooled while A_s and A_f denote the temperatures of the start (0%) and finish (100%) of the austenite phase upon being heated and M_d is a high temperature above which the alloy loses its distinct properties that were mentioned earlier [21].

Upon plastic deformation in the martensite phase, SMAs behave like any other metal except that they have a memory of their unique austenite form and, upon being heated beyond A_f but below M_d , they undergo a temperature-induced phase transformation from martensite to austenite and return to the unique initial form even if cooled again afterward. This type of actuation requires active control, where batteries are usually used to increase the temperatures and induce this shape memory effect through ohmic heat. Meanwhile, upon plastic deformations at temperatures above A_f but below M_d , SMAs undergo a stress-induced phase transformation from austenite to martensite. This leads to elastic and super-elastic deformations that are both reversible because the simple removal of the stress is enough to return the alloy to the austenite phase and therefore its initial shape [22].

It is noted that using SMAs as coils instead of wires increases the deformation attainability from 5% to between 200% and 1600% depending on multiple factors related to the material properties and spring dimensions [23].

A. Objective

After obtaining the required torque at the ankle joint, the material properties and the dimensions of the spring can be selected so that they fit the profile of the recorded gait. On the basis of several literature reviews, it is theorized that increasing the stiffness continuously while walking is more effective than using a spring with constant stiffness [7][8]. This theorization is based on biomimicry; i.e., biological tissues around the ankle have stiffnesses that are not constant but rather increase rapidly with respect to stretch [24]. This demonstrates that a spring made from traditional material would not function appropriately and a variable-stiffness AFO would be more biologically accepted. The stiffness during the gait is usually changed using an active AFO by integrating motors or pneumatics into the system, which raises the issues of bulkiness and heaviness. A new and more favorable approach would be to utilize the super-elastic property of SMAs that was introduced in the previous section.

Although the equations of normal springs have been adapted to SMA springs by varying the shear modulus, that approach is inaccurate owing to the recoverability of SMA even at a shear strain of 6%–8% and not only in the elastic phase. Furthermore, the detwinning effect on the spring elongation is not considered, which limits the use of the material. Therefore, the objective of this section is to calculate the spring requirements needed to exert the maximum AFO force that was previously calculated using the static two-state model [23] and thus describe the relation between the SMA spring dimensions and the mechanical properties of the spring for the selection of the optimal spring attributes. Lightness and compactness are desirable, and the model was thus altered and implemented in an optimization algorithm with the goal of finding the smallest springs that realize this force.

B. Methodology

The austenite phase was considered for the calculations. Furthermore, because the SMA has multiple grades, each with its own material properties, the variables in the optimization algorithm were the dimensions, material properties, and number of SMA springs of the spring mechanism. Meanwhile, the constraints were the maximum force required, the ranges of available mechanical properties, and the ranges of manufacturable spring dimensions needed to have a logical and viable system. The algorithm is illustrated as a flow chart in Fig. 6. The considered variables and constraints are summarized in Table 1.

The procedure starts by selecting the SMA material properties according to the commercially available products and then choosing the desired maximum shear stress; i.e., specifying the factor of safety. In this step, the desired and critical maximum shear stresses were considered equal because a factor of safety will be set in later steps. The diameter of the spring wire d is calculated as

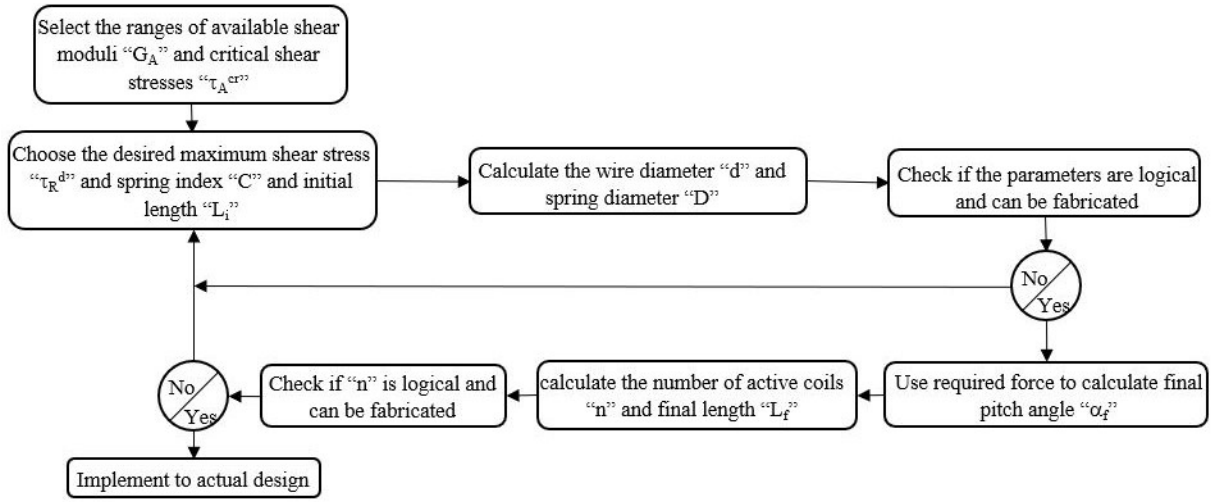


Fig. 6. Flow chart of the SMA optimization algorithm

TABLE I. VARIABLES AND CONSTRAINTS OF THE SMA OPTIMIZATION ALGORITHM

| Variables | Constraints |
|--|---------------|
| Shear modulus of Austenite, G_A | 25 to 40 GPa |
| Critical shear stress of 100% Austenite, τ_A^{cr} | 60 to 460 MPa |
| Spring index, C | 4 to 12 |
| Initial length, L_i | 50 to 150 mm |

$$d = \sqrt[4]{8CF/\pi\tau_A^{cr}}, \quad (1)$$

where C is the spring index, τ_A^{cr} is the desired maximum shear stress, and F is the exerted force, which is the maximum force that should be supplied by the device as calculated in the previous section.

The spring diameter D can then be simply calculated from the spring index and wire diameter as

$$D = Cd. \quad (2)$$

These diameters were checked to verify the manufacturability of the spring. After verification, the initial length L_i and initial pitch angle α_i were selected and used with the shear modulus of austenite G_A to calculate the final pitch angle α_f and the number of turns n as

$$8FD^2/\pi G_A d^4 \cos^2 \alpha_i = (1 + \nu)(\sin \alpha_f - \sin \alpha_i) / \cos^2 \alpha_f (1 + \nu \cos^2 \alpha_f), \quad (3)$$

$$n = L_i / (\pi D \tan \alpha_i + d). \quad (4)$$

The final length of the spring L_f was calculated to check if it was applicable:

$$L_f = n(\pi D \cos \alpha_f \tan \alpha_i / \cos \alpha_i + d). \quad (5)$$

Poisson's ratio ν was set to a constant of 0.33 and Young's modulus E was calculated as

$$E = 2(1 + \nu)G. \quad (6)$$

Identical SMA springs were placed in parallel so that the force was divided equally among them; the number of springs is denoted N .

For a more robust and accurate description of the SMA spring behavior, one can also use the martensite force equation after the beginning of the phase shift. This process describes the force of the spring depending on the volumetric ratio of martensite in the alloy. The details of the calculation are given in the appendix.

C. Results

For the previously mentioned force F , the optimization algorithm yielded six SMA springs. Each spring had an initial length of 8 cm. The wire diameter was 2 mm and the spring diameter was 8 mm. The initial pitch angle was 0.0175 rad (1°) and there were 36 turns. Each of the springs would have to be elongated by 3.7 cm to reach a final length of 11.7 cm and exert a force of 190 N to account for 100% of the biological ankle torque. However, according to the maximum foot angle in the stance, the elongation can only reach a maximum of 2.3 cm. Therefore, reversing the previous process and starting with a constant maximum elongation of 2.3 cm, the six springs would have a final length of 10.3 cm, a final pitch angle of 0.0454 rad (2.6°), and a force of 115 N per spring. This would increase the factor of safety of the spring from 1 to 1.6. According to An, S. [23], this factor of safety should not be too close to 1 or else the system becomes susceptible to breaking down and it should not be too far from 1 or else the system becomes inefficient. We therefore consider a factor of safety of 1.6 to be suitable.

This device is expected to lower the biological ankle torque required for locomotion from 67 to 26 N for our participant. Thus, reducing the forces exerted by the calf muscles brings the effectiveness of the AFO to 61%.

IV. CONCLUSION

The lightweight design of the proposed AFO has the potential of reducing the required muscle forces during

walking by up to 61% and consequently reducing the metabolic energy cost of locomotion. The SMA used for the spring material gives the device higher biocompatibility relative to similar designs. Finally, this device works similarly to the Achilles tendon; therefore, from a biomedical point of view, we expect such a concept to be beneficial for rehabilitating patients suffering from Achilles tendon rupture, which will be investigated in future work.

V. APPENDIX

In this paper, the authors used the force equation of the austenite phase (3) to predict the behavior of the SMA spring throughout the locomotion process. It is noted that this method can be further enhanced using the martensite equation (7) after the phase-shift begins, which depends on the instantaneous detwinned martensite volume fraction ε_{ST} and residual strain of the material. The martensite equation is

$$8D^2/\pi G_M d^4 \cos^2 \alpha_i (F + \pi d^3 G_M \gamma_L \varepsilon_{ST}) = (1 + \nu)(\sin \alpha_f - \sin \alpha_i) / \cos^2 \alpha_f (1 + \nu \cos^2 \alpha_f), \quad (7)$$

where G_M is the shear modulus of martensite and γ_L is the maximum residual strain.

ACKNOWLEDGMENT

We thank Edanz (<https://jp.edanz.com/ac>) for editing a draft of this manuscript.

REFERENCES

- [1] K. E. Zelik, T.-W. P. Huang, P. G. Adamczyk, and A. D. Kuo, "The role of series ankle elasticity in bipedal walking," *J. Theor. Biol.*, vol. 346, pp. 75–85, 2014.
- [2] S. H. Collins, M. B. Wiggins, and G. S. Sawicki, "Reducing the energy cost of human walking using an unpowered exoskeleton," *Nature*, vol. 522, no. 7555, pp. 212–215, 2015.
- [3] W. Herzog, "Why are muscles strong, and why do they require little energy in eccentric action?," *J. Sport Health Sci.*, 2018.
- [4] G. S. Sawicki, C. L. Lewis, and D. P. Ferris, "It pays to have a spring in your step," *Exerc. Sport Sci. Rev.*, vol. 37, no. 3, pp. 130–138, 2009.
- [5] F. H. Abadi, T. A. Muhamad, and N. Salamuddin, "Energy expenditure through walking: Meta analysis on gender and age," *Procedia Soc. Behav. Sci.*, vol. 7, pp. 512–521, 2010.
- [6] F. S. Shahar et al., "A review on the orthotics and prosthetics and the potential of kenaf composites as alternative materials for ankle-foot orthosis," *J. Mech. Behav. Biomed. Mater.*, vol. 99, pp. 169–185, 2019.
- [7] M. K. Shepherd, A. F. Azocar, M. J. Major, and E. J. Rouse, "Amputee perception of prosthetic ankle stiffness during locomotion," *J. Neuroeng. Rehabil.*, vol. 15, no. 1, p. 99, 2018.
- [8] M. K. Shepherd, A. F. Azocar, M. J. Major, and E. J. Rouse, "The difference threshold of ankle-foot prosthesis stiffness for persons with transtibial amputation," in *2018 7th IEEE International Conference on Biomedical Robotics and Biomechatronics (Biorob)*, 2018.
- [9] B. Chen, B. Zi, Y. Zeng, L. Qin, and W.-H. Liao, "Ankle-foot orthoses for rehabilitation and reducing metabolic cost of walking: Possibilities and challenges," *Mechatronics (Oxf.)*, vol. 53, pp. 241–250, 2018.
- [10] W. Chen, S. Wu, T. Zhou, and C. Xiong, "On the biological mechanics and energetics of the hip joint muscle-tendon system assisted by passive hip exoskeleton," *Bioinspir. Biomim.*, vol. 14, no. 1, p. 016012, 2018.
- [11] Y. T. Wang, D. D. Pascoe, C. K. Kim, and D. Xu, "Force patterns of heel strike and toe off on different heel heights in normal walking," *Foot Ankle Int.*, vol. 22, no. 6, pp. 486–492, 2001.
- [12] T. J. Roberts and N. Konow, "How tendons buffer energy dissipation by muscle," *Exerc. Sport Sci. Rev.*, vol. 41, no. 4, pp. 186–193, 2013.
- [13] L. Deberg, M. Taheri Andani, M. Hosseini-pour, and M. Elahinia, "An SMA passive ankle foot orthosis: Design, modeling, and experimental evaluation," *Smart Mater. Res.*, vol. 2014, pp. 1–11, 2014.
- [14] L. Vargas-Valencia, A. Elias, E. Rocon, T. Bastos-Filho, and A. Frizzera, "An IMU-to-body alignment method applied to human gait analysis," *Sensors (Basel)*, vol. 16, no. 12, p. 2090, 2016.
- [15] S. Plagenhoef, F. G. Evans, and T. Abdelnour, "Anatomical data for analyzing human motion," *Res. Q. Exerc. Sport*, vol. 54, no. 2, pp. 169–178, 1983.
- [16] W. T. Dempster and G. R. L. Gaughran, "Properties of body segments based on size and weight," *Am. J. Anat.*, vol. 120, no. 1, pp. 33–54, 1967.
- [17] S.-S. Ko, J.-S. Chung, and W.-Y. So, "Correlation between waist and mid-thigh circumference and cardiovascular fitness in Korean college students: a case study," *J. Phys. Ther. Sci.*, vol. 27, no. 9, pp. 3019–3021, 2015.
- [18] T. Kokot, E. Malczyk, E. Ziólko, M. Muc-Wierzoń, and E. Fatyga, "Assessment of nutritional status in the elderly," in *Nutrition and Functional Foods for Healthy Aging*, Elsevier, 2017, pp. 75–81.
- [19] M. Grimmer, M. Eslamy, and A. Seyfarth, "Energetic and peak power advantages of series elastic actuators in an actuated prosthetic leg for walking and running," *Actuators*, vol. 3, no. 1, pp. 1–19, 2014.
- [20] L. Case, Z. Kreiner, J. Redmond, B. Trease, *Shape Memory Alloy Shape Training Tutorial*. Fall 2004.
- [21] R. Boyer, Ed., *Materials properties handbook: Titanium alloys*. ASM International, 1994.
- [22] H. Qian, H. Li, G. Song, and W. Guo, "Recentering shape memory alloy passive damper for structural vibration control," *Math. Probl. Eng.*, vol. 2013, pp. 1–13, 2013.
- [23] S.-M. An, J. Ryu, M. Cho, and K.-J. Cho, "Engineering design framework for a shape memory alloy coil spring actuator using a static two-state model," *Smart Mater. Struct.*, vol. 21, no. 5, p. 055009, 2012.
- [24] M. K. Shepherd and E. J. Rouse, "Design of a quasi-passive ankle-foot prosthesis with biomimetic, variable stiffness," in *2017 IEEE International Conference on Robotics and Automation (ICRA)*, 2017.